Scientific paper

Self-assembled Organogels Formed by L-Leucine Dihydrazide Derivative

Yang Yu,[1,2] Ning Song,[2] Shen Jin,[2] Wei Shi,[3] Yuchun Zhai[1] and Chuansheng Wang[2,*]

[1] *School of Materials and Metallurgy, Northeastern University, Shenyang 110004, China*

[2] *Shenyang University of Chemical Technology, Shenyang 100142, China*

[3] *TangShan SanYou Chemical Industries Co., Ltd, Tangshan 063305, China*

* *Corresponding author: E-mail: wchsh18@163.com*

Received: 21-01-2013

Abstract

A new organogelator, benzyl (4-methyl-1-oxo-1-(2-hexadecanoylhydrazinyl)pentan-2-yl)carbamate (designated as Cbz-Leu-HdHz), was designed and synthesized, which could self-assemble in many organic solvents and form the thermally reversible physical supramolecular organogels. The gel-sol phase transition temperatures (T_{GS}) were determined as a function of gelator concentration and the corresponding enthalpies (ΔH_g) were extracted. SEM, FT-IR and XRD were used for the investigations of the morphology and formation mechanism of organogels in the presence of the Cbz-Leu-HdHz. Based on the XRD data and molecular modeling, it was possible to propose packing modes for the formation of organogelator aggregates.

Keywords: Hydrogen bonding, L-leucine, organogel, organogelator, self-assembly.

1. Introduction

In recent years low-molecular-mass organogelators (LMOGs) and their thermally reversible organogels have received increasing attention due to their unique features and potential applications.[1–3] The LMOGs exhibit interesting self-assembly phenomena and form three-dimensional (3D) networks. Owing to their unique behavior, the development of inexpensive and efficient organogelators is of great interest. They could be applied in a wide-range of industrial fields, which includes cosmetics, chiral chromatography and nanotechnology development such as optoelectronics, photovoltaics,[4–6] as well as in the areas like drug delivery,[7–11] tissue engineering,[12–14] sensing and soft lithography, etc.[15]

Generally speaking, these organogels are materials which consist of an organic liquid and a small amount of LMOG.[16] The gelator molecules self-assemble into nanoscale superstructures, such as fibers, rods, ribbons and sheets through hydrogen bonding, π–π stacking, van der Waals' forces, coordination and charge-transfer interactions to create 3D networks which lead to the gelation of organic solvents.[17] In amide compounds, such as amino acids,[18–22] urea [23–25] and dihydrazide derivatives,[26] hydrogen bonding is for gelation. In the recent years, some gellators, which can be prepared easily and at low cost, have been reported to show good gelation ability for many organic solvents and oils,[27–28] such as small peptides or pseudo-peptides[23,29–31] and *N*-lauroyl L-alanine (LA) and *N*-stearoyl L-alanine (SA) were obtained after alkaline hydrolysis of the methyl ester derivatives.[32] Despite the numerous trends in gelling process as well as the impressive variety of gelators, it is difficult to predict the molecular structure of a potential gelator.

To further this research, we have developed a new chiral gelator benzyl (4-methyl-1-oxo-1-(2-hexadecanoylhydrazinyl)pentan-2-yl)carbamate (Cbz-Leu-HdHz (**5**) on) based on the L-leucine and cetane hydrazide derivative, which can assemble through intermolecular interactions such as hydrogen bonding and complementary hydrophobic interactions in solution induce the gelation of organic solvents. We studied their gelling behaviors in different organic solvents and investigated the strength of the resulting gels by using the dropping ball method. The results showed that the gelator has excellent gelation ability in many organic solvents. Infrared spectroscopy (FT-IR) was used to study the driving forces of intermolecular interactions of the gelator to form gels. Scanning electron microscopy (SEM) revealed a great difference of xerogel

in different solvents, besides providing a comparative visual technique to assess the impact of the spacer unit on the mode of self-assembly. The results from X-ray diffraction (XRD) showed that wet gel, xerogel and gelator had different crystalline states. On the basis of XRD data, we discuss the possible model of aggregation of Cbz-Leu-HdHz.

2. Experimental

2. 1. Materials and Methods

L-Leucine methyl ester hydrochloride (**1**), carbobenzoxy chloride (Cbz-Cl) and *n*-hexadecanoyl chloride (**4**) were purchased from Yangzhou Baosheng Biochemical Co., Ltd. Hydrazine hydrate was obtained from Tianjin Bodi Chemical Co., Ltd. The other chemicals were of the highest commercial grade available and used without further purification. All solvents used in the syntheses were purified, dried, or freshly distilled to meet the experimental requirement.

FT-IR spectra were recorded on a Nicolet Nexus 470. ^{1}H NMR spectra were recorded with a Bruker Avance 600 MHz spectrometer. Melting points were determined by a Fukai X-4 digital melting point instrument. SEM images were obtained by the JEOL JSM-6360LV scanning electron microscope, the accelerating voltage was 10 kV and the emission was 10 mA. The samples for SEM were prepared in a 0.5 mL bottle and frozen in liquid nitrogen. The frozen samples were evaporated by a vacuum pump, and then the dried samples were coated by gold. XRD was performed by a Bruker D8 ADVANCE instrument using CuKα radiation in steps of 0.05°. The preparation of sample was similar to that of the SEM samples.

The critical gelation concentration (CGC) was studied and confirmed by the inverted test tube method.[33] When the tube can be inverted without fluid, we judged it žgelation'. Thermal stabilities of the gels were studied by the dropping ball method.[34]

2. 2. Synthesis of 5

The synthetic route for L-leucine-based organogelator **5** is shown in Scheme 1.

Step 1: L-Leucine methyl ester hydrochloride (methyl 2-amino-4-methylpentanoate, **1**) (8.17 g, 45 mmol) was dissolved in saturated aqueous Na_2CO_3; then benzyloxycarbonyl chloride (Cbz-Cl) (7.65 g, 45 mmol) was slowly added to this solution and stirred at room temperature for 16 h. The solution was extracted by diethyl ether for three times (3 × 30 mL), the combined organic phase was washed by 0.01 mol/L HCl (100 mL) solution and dried over anhydrous $MgSO_4$ for 2 h. After filtration, the solvent was removed by evaporation under reduced pressure. Finally, the oily liquid of Cbz-L-Leu-OMe (**2**) was obtained.

Step 2: A mixture of **2** (6.80 g, 24 mmol) and hydrazine hydrate (4.57 g, 90 mmol) was dissolved in methanol (100 mL) and stirred at room temperature continuously for 16 h; the solvent was removed under reduced pressure; the residue was dissolved in chloroform (100 mL); the solution was thoroughly washed three times with brine (3 × 30 mL), and dried over anhydrous $MgSO_4$ for 2 h. After filtration, the solvent was removed under reduced pressure to obtain the white solid hydrazide **3**.

Step 3: Hydrazide **3** (6.15 g, 22 mmol) and *n*-hexadecanoyl chloride (**4**) (6.40 g, 23 mmol) were dissolved in chloroform; the mixture was stirred at room temperature for 6 h; the volatile components were removed under reduced pressure and then solid product was three times recrystallized from methanol to obtain the pure product **5** in a yield above 80%.

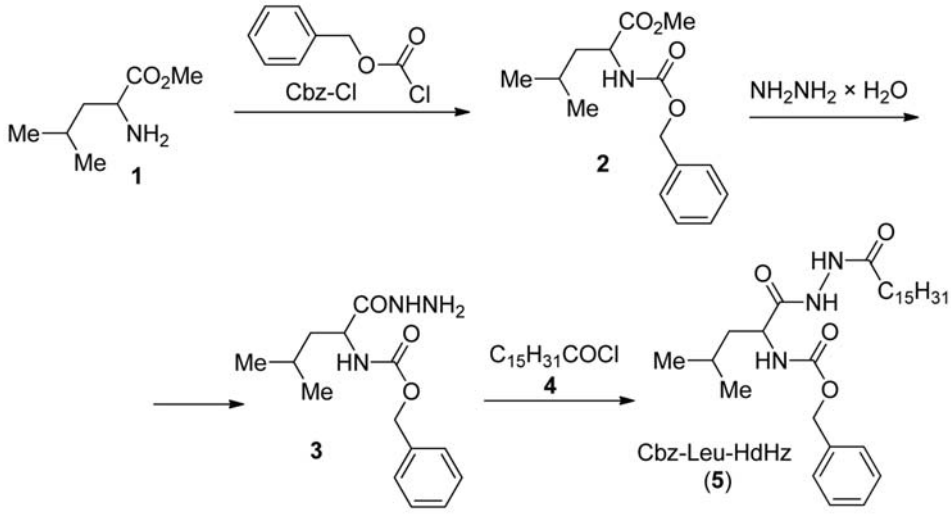

Scheme 1. The synthetic route to Cbz-Leu-HdHz (**5**).

2. 3. Characterization of 5

FT-IR (KBr) ν 3290 (N–H, amide A), 3220 (N–H, amide A), 3032, 2956, 2920, 2850, 1690 (C=O), 1670, 1600 (C=O, amide I), 1540 (N–H, amide II), 1460, 1283, 1264, 1204, 1111, 1043, 975, 721, 696, 649, 563 cm^{-1}.

^{1}H NMR (600 MHz, DMSO-d_6) ä 9.84 (s, 1H, N*H*CO(CH_2)$_{14}$), 9.69 (s, 1H, Leu-NH), 7.42 (d, 1H, J = 8.2 Hz, Cbz-NH), 7.39–7.17 (m, 5H, Ph-H), 5.01 (s, 2H, Ph-CH_2), 4.11 (s, 1H, *CH*CH_2CH(CH_3)$_2$), 2.08 (t, H, J = 7.1 Hz, C*H*$_2$(CH_2)$_{13}CH_3$), 1.66 (s, 1H, C*H*(CH_3)$_2$), 1.49 (s, 4H, C*H*$_2$(CH_2)$_{12}CH_3$, C*H*$_2$CH(CH_3)$_2$), 1.24 (s, 24H, CH_2(*CH*$_2$)$_{12}CH_3$), 0.92–0.79 (m, 9H, 3 × CH_3).

LC-MS (ESI): *m/z* 540.8 $[M+Na]^+$, 535.9 $[M+NH_4]^+$ and 518.7 $[M+H]^+$.

mp: 124–125 °C.

3. Results and Discussion

3. 1. Gelation Properties

A weighted amount of gelator **5** was weighted and a selected organic solvent (2 mL) was added, the solution was heated in a sealed test tube (15 mm in diameter) until becoming clear, and then stored at 25 °C for 2–6 h. If there was no fluid in the test tube when turned upside down, the organogel has formed. In a given solvent, gelation occurred at a critical concentration, which is called critical gelation concentration (CGC). Table 1 summarizes the gelation behavior of Cbz-Leu-HdHz (**5**) in various solvents. It was found that Cbz-Leu-HdHz (**5**) (at concentration < 3.0 wt %) could form stable organogels in many solvents, such as vegetable oil, 1,2-dichloroethane, *n*-octane, esters, *n*-pentanol, CCl_4, cyclohexane, *n*-hexanol, etc. These gels were stable toward shaking and they were also stable for a few weeks at room temperature (25 °C). It also indicated that Cbz-Leu-HdHz (**5**) acted as a versatile gelator for various organic solvents. However, this gelator **5** cannot gelatinize DMF, methanol, ethanol, acetone and chloroform, maybe their strong polarity destroys the hydrogen bonding interactions between amide-amide groups. Generally, the gelation ability of the gelator was related to the interaction between gelator and solvent molecules, governed by molecular polarity and the respective structural factors. So, it is implied that some relationship exists between polarity, aromaticity, and gelation ability, although the gel stability was directly proportional to the concentration of the gelator.[35]

The organogels formed by Cbz-Leu-HdHz (**5**) are variable in color, such as white opaque for ethylene glycol gels (CGC = 0.47 wt %), light yellow transparent for castor oil gels (CGC = 0.73 wt %) and completely transparent for 1,2-dichloroethane gel (CGC = 1.12 wt %). In addition, Cbz-Leu-HdHz (**5**) dissolved in butyl acetate (CGC = 1.87 wt %) and ethyl acetate (CGC = 2.15 wt %) formed white opaque gels. According to previous work,[36] it is assumed that the optical aspect is related to the crystallinity of the gels.

3. 2. Gel Stability Studies

In this test, a small stainless steel ball (diameter 3 mm) was placed on the top of the gel in a test tube (10 mm diameter). The tube was slowly heated (1 °C min^{-1}) in a thermostatic oil bath until the ball fell from the surface of the gel to the bottom of the tube. The temperature at this point was recorded. The whole procedure was repeated three times and the average temperature was taken as the T_{GS} of the system. However, the gelation ability was not affected, which suggested that these organogels possess thermoreversible properties.

From our results we know that the thermal stabilities of these gels increase upon increasing the concentration of the gelator in different solvents. The gel-sol phase transition temperatures (T_{GS}) of Cbz-Leu-HdHz (**5**) in ethylene glycol, 1,2-dichloroethane and chlorobenzene are plotted against the gelation concentration in Figure

Table 1 Gelation ability of Cbz-Leu-HdHz (**5**) in organic solvents

Solvent	CGC	State	Solvent	CGC	State	ΔH_g / kJ mol^{-1}
soybean oil	0.98	TG	chlorobenzene	1.98	TG	30.00
castor oil	0.73	TG	ethylene glycol	0.47	OG	138.10
olive oil	0.88	TG	*n*-pentanol	2.47	OG	
benzene	2.99	OG	*n*-hexanol	2.61	OG	
toluene		P	ethyl acetate	2.15	OG	
chloroform		P	butyl acetate	1.87	OG	
acetone		P	cyclohexane	2.50	OG	
p-dioxane	2.98	OG	tetrachloromethane	2.32	OG	
DMF		Sol	1,2-dichloroethane	1.12	TG	33.14
ether		Ins	*n*-octane	1.59	OG	

Note: critical gelation concentration in wt % (CGC, wt %). TG: transparent gel; OG: opaque gel; P: partial gelation; Sol: solution; Ins: insoluble (not fully soluble at 3.0 wt %).

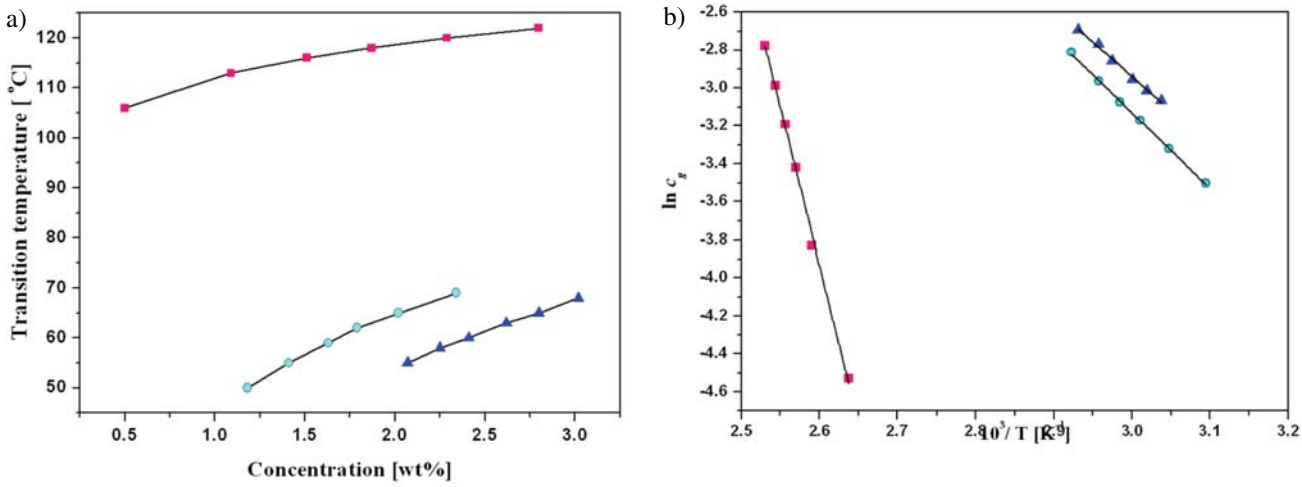

Figure 1. (a) T_{GS} as a function of concentration of Cbz-Leu-HdHz (**5**) and (b) van't Hoff plots of Cbz-Leu-HdHz (**5**) in ethylene glycol (■), 1, 2-dichloroethane (○) and chlorobenzene (▼), respectively.

1a. The thermodynamic analysis for the gel-sol transition was carried out by using a van't Hoff relationship. From the relationship between T_{GS} and the corresponding concentration, the gel-sol transition enthalpy (ΔH_g) was determined from the slope of ln c_g versus $(T_{GS})^{-1}$. The plots are represented in Figure 1b and the resulting enthalpy values in various solvents are summarized in Table 1.

3. 3. Scanning Electron Microscopy (SEM) Studies

To gain visual insight into the morphologies of the aggregates, the xerogels prepared by freeze-drying of gels prepared by **5** in CCl_4, cyclohexane and butyl acetate were studied by SEM. As shown in Figure 2a, the gelator self-assembled into a bunch of curly flake aggregates with the minimum thickness of dozens of nanometers and width of several micrometers. Figure 2b represents the aggregates structure, which looks like hemp rope, section by section, intertwined with each other, the thinnest being more than 200 nm, the thickest more than one micrometer. On the other hand, Figure 2c exhibits a sheet aggregation mode, with some ribbon structure. The sheets are longer than 6 μm, wider than 4 μm and as thick as hundreds of nanometers.

Previous research has shown[36] that the light transmittance of a gel depends upon its crystallinity, and the nature of the solvent can affect the degree of disorder of a gel. From the research of morphology, we can see that the gelator has self-assembled into 3D structure but the aggregates are different in various solvents. Despite all the aggregates differences, they have got two things in common: larger size and lower porosity. From Table 1 we can see that the Cbz-Leu-HdHz (**5**) in organic solvents can form gels but requires higher CGC and most of the resulting gels are opaque gels, this may be caused by the same reason as described above.

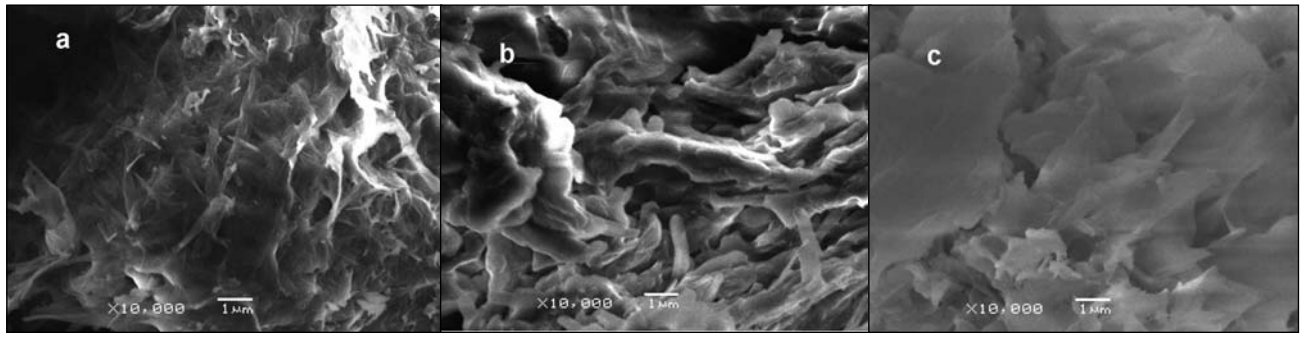

Figure 2. SEM images of Cbz-Leu-HdHz (**5**) xerogels formed by (a) 3.0 wt % in CCl_4, (b) 2.5 wt % in cyclohexane, and (c) 2.3 wt % in butyl acetate. Magnitudes are 10,000×, respectively.

3. 4. FT-IR Measurements Studies

We measured the FT-IR spectra to evaluate the driving forces for gelation. Figure 3 shows the FT-IR spectra of Cbz-Leu-HdHz (**5**) in 1,2-dichloroethane solution and in 1,2-dichloroethane gel respectively. In 1,2-dichloroethane solution, the typical IR bands, arising from non-hydrogen bonded amide groups, were observed at 3290, 3221 cm^{-1} (amide A), 1690 cm^{-1} (amide I), and 1541 cm^{-1} (amide II). The IR spectra of 1,2-dichloroethane gel showed the bands at 3280, 3218 cm^{-1} (amide A), 1647 cm^{-1} (amide I), and 1535 cm^{-1} (amide II), characteristic for hydrogen bonded amide groups. In addition, the IR bands of urethane group appeared at 1670 cm^{-1} in 1,2-dichloroethane solution and 1687 cm^{-1} in 1,2-dichloroethane gel. Such IR shifts indicate the formation of the intermolecular hydrogen bonding interaction between the amide and the urethane groups.[37–40]

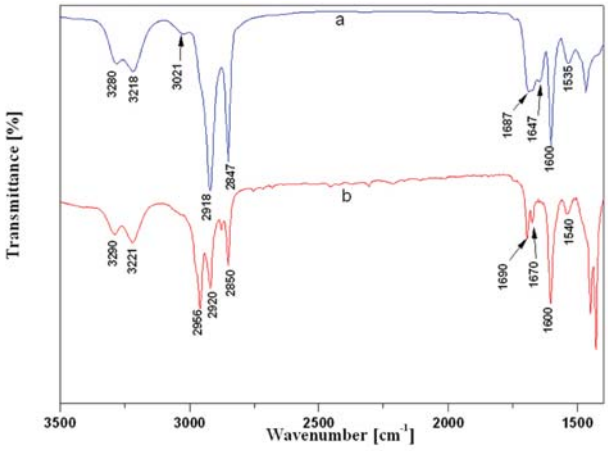

Figure 3**.** FT-IR spectra, (a) 1,2-dichloroethane gel of Cbz-Leu-HdHz (**5**) (1.39 wt %) and (b) 1,2-dichloroethane solution of Cbz-Leu-HdHz (**5**) (0.44 wt %).

Furthermore, in 1,2-dichloroethane gel the absorption bands of the antisymmetric (ν_{as}) and symmetric (ν_s) stretching vibration appeared at low wave numbers, 2918 cm^{-1} (ν_{as} C–H) and 2847 cm^{-1} (ν_s C–H), comparable with those of the analogous Cbz-Val-HdHz in 1,2-dichloroethane solution. These suggests that the alkyl groups of Cbz-Leu-HdHz (**5**) are organized in a self-assembled nanostructure via hydrophobic interactions.[26, 37] The results indicate that the driving forces for the formation of the organogel are mainly hydrogen bonding and complementary hydrophobic interactions.

3. 5. X-Ray Powder Diffraction (XRD) Studies

The XRD pattern of tetrachloromethane wet gel is shown in Figure 4. Accordingly, this wet gel is amorphous as shown by the broad peak form of its X-ray diffraction pattern; this may be due to the heavy scattering of the solvent molecules, although the whole state of the gel forms an orderly network structure.

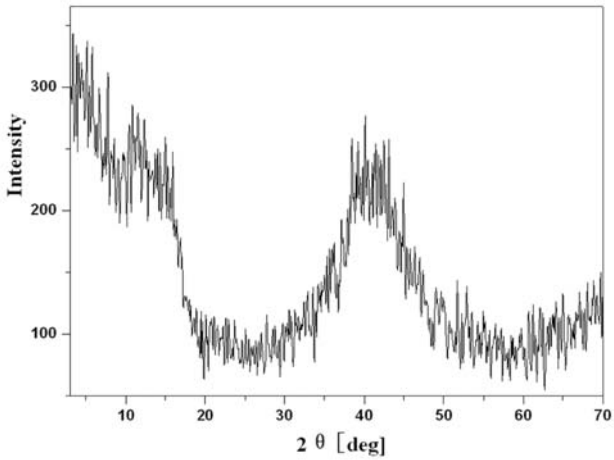

Figure 4. X-Ray powder diffraction patterns of CCl_4 wet gel of Cbz-Leu-HdHz (4.0 wt %).

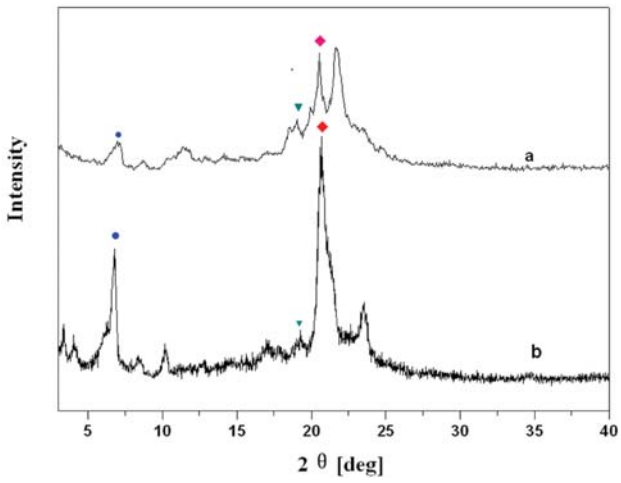

Figure 5. X-Ray powder diffraction patterns of (a) Cbz-Leu-HdHz (**5**) solid and (b) CCl_4 xerogel of Cbz-Leu-HdHz (**5**) (3 wt %). The marked peaks in (a) and (b) represent three diffraction peaks existing in both cases.

The XRD of CCl_4 xerogel is shown in Figure 5; the diffraction peaks are sharper and the signal-to-noise ratio (SNR) is higher comparing with the wet gel, the results demonstrating that the xerogel is a very good crystal material. Although some diffraction peaks of dried gel have similar position to those of the gelator of Cbz-Leu-HdHz (Figure 5), they belong to different crystalline state. Just in virtue of the intermolecular interaction by the solvent, the gelator has been rearranged by self-assembly during gelation.

3. 6. Molecular Model of a Xerogel

Figure 6 shows the sharp peak at small-angles in the XRD of the xerogel which is attributed to the sheet organization of the Cbz-Leu-HdHz (**5**) aggregates. From the optimized HyperChem 8.0 model (Semi-empirical-INDO method, Polak–Ribiere algorithm), the length of the long alkyl chain (i.e. $C_{15}H_{31}$) of Cbz-Leu-HdHz (**5**) is 1.95 nm, whereas the length of the whole Cbz-Leu-HdHz (**5**) molecule is 2.42 nm (Figure 7a). The Bragg distance (*d*) of the xerogel of Cbz-Leu-HdHz (**5**) is 5.13 nm as shown by the XRD measurements. XRD and FT-IR data indicate the existence of gel aggregates that consist of a repeating bilayer unit, which bears the head-to-head packing model with highly tilted alkyl chains relative to the bilayer normal. Within the bilayer unit, the amphiphiles are connected by intra- and inter-layer hydrogen bonds to form a hydrogen bonded network. For the random arrangement of the bilayer unit, the possible modes are shown in Figure 7b.

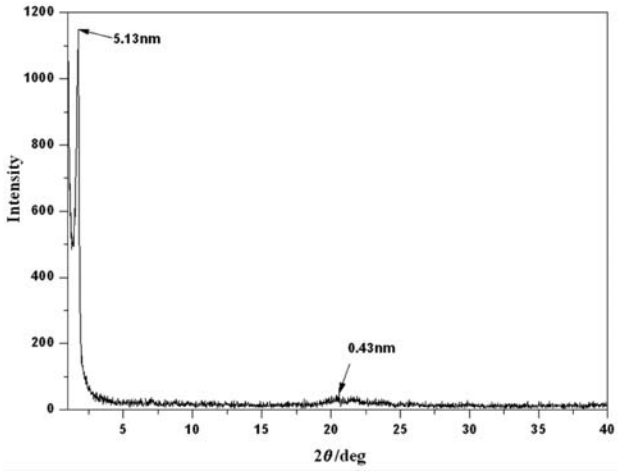

Figure 6. X-Ray powder diffraction pattern of the cyclohexane xerogel of Cbz-Leu-HdHz (**5**) (2.5 wt %).

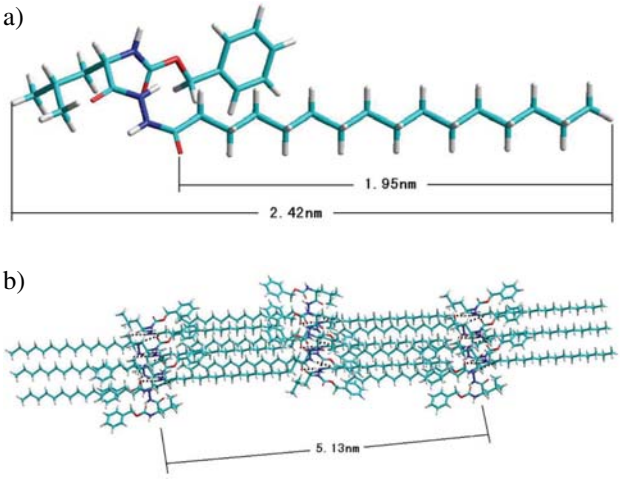

Figure 7. Energy-minimized structures of Cbz-Leu-HdHz (**5**) and a possible model for the aggregates in organic solvents. Dashed lines represent hydrogen bonding interactions.

4. Conclusions

In this paper, we describe the synthesis and gelation properties of a new gelator based on L-leucine methyl ester hydrochloride. Through studying the gelling behaviors, we have proved that L-leucine dihydrazide derivative **5** is an excellent gelator. The gelator can in the presence of various organic solvents self-assemble into orderly three-dimensional network structures, such as fibers, rods, ribbons and sheets nanostructures. The state of aggregation may influence transparency of the gel. We also found out that the driving forces for the organogelation are mainly hydrogen bonding interactions between the amide groups and complementary hydrophobic interactions of the alkyl chains. Finally, we deduced the simulated molecular structure by the energy minimization and its possible model of aggregation. Further work is being carried out in this laboratory in particular towards the application of such organogels in drug delivery.

5. Acknowledgment

This research is supported by the National Natural Science Foundation of China (No. 30772670).

6. References

1. W. J. Zhao, Y. Y. Li, T. Sun, H. Yan, A. Y. Hao, F. F. Xin, H. C. Zhang, W. An, L. Kong, Y. M. Li, *Colloids Surf., A* **2011**, *374*, 115–120.
2. T. H. Kim, D. G. Kim, M. J. Lee, T. S. Lee, *Tetrahedron* **2010**, *66*, 1667–1672.
3. D. J. Abdallah, R. G. Weiss, *J. Braz. Chem. Soc*. **2000**, *11*, 209–218.
4. D. J. Abdallah, R. G. Weiss, *Adv. Mater*. **2000**, *12*, 1237– 1247.
5. P. Terech, R. G. Weiss, *In Surface Characterization Methods: Principles, Techniques, and Applications;* Milling, A. J. (ed), CRC Press: New York, **1999**, ch. 10.
6. J. van Esch, F. Schoonbeek, M. de Loos, E. M. Veen, R. M. Kellogg, B. L. Feringa, *Supramolecular Science: Where It Is and Where It Is Going*; *NATO ASI Series C, Mathematical and Physical Sciences*; R. Ungaro (ed), Kluwer Academic Publishers: Dordrecht; Boston; **1999**, *527*, 233–260.
7. M. Shirakawa, N. Fujita, T. Tani, K. Kaneko, S. Shinkai, *Chem. Commun*. **2005**, 4149–4151.
8. P. K. Vemula, J. Li, G. J. John, *J. Am. Chem. Soc.* **2006**, *128*, 8932–8938.
9. A. Friggeri, B. L. Feringa, J. van Esch, *J. Controlled Release* **2004**, *97*, 241–248.

10. J. C. Tiller, *Angew. Chem., Int. Ed*. **2003**, *42*, 3072–3075.
11. S. Sahoo, N. Kumar, C. Bhattacharya, S. S. Sagiri, K. Jain, K. Pal, S. S. Ray, B. Nayak, *Des. Monomers Polym.* **2011**, *14*, 95–108.
12. X. M. Wang, A. Horri, S. G. Zhang, *Soft Matter* **2008**, *4*, 2388–2395.
13. R. G. Ellis-Behnke, Y.-X. Liang, S.-W. You, D. K. C. Tay, S. Zhang, K.-F. So, G. E. Schneider, *Proc. Natl. Acad. Sci. USA* **2006**, *103*, 5054–5059.
14. K. Y. Lee, D. J. Mooney, *Chem. Rev.* **2001**, *101*, 1869–1880.
15. S. J. Jhaveri, J. D. McMullen, R. Sijbesma, L.-S. Tan, W. Zipfel, C. K. Ober, *Chem. Mater*. **2009**, *21*, 2003–2006.
16. M. George, R. G. Weiss, *Langmuir* **2003**, *19*, 1017–1025.
17. C. Y. Bao, R. Lu, M. Jin, P. C. Xue, C. H. Tan, Y. Y. Zhao, G. F. Liu, *Carbohydr. Res.* **2004**, *339*, 1311–1316.
18. D. K. Smith, F. Diederich, *Chem. Eur. J.* **1998**, *4*, 1353–1361.
19. C. S. Love, A. R. Hirst, V. Chechik, D. K. Smith, I. Ashworth, C. Brennan, *Langmuir* **2004**, *20*, 6580–6585.
20. C. Kim, K. T. Kim, Y. Chang, *J. Am. Chem. Soc*. **2001**, *123*, 5586–5587.
21. H. F. Chow, J. Zhang, *Tetrahedron* **2005**, *61*, 11279–11287.
22. G. Palui, F. X. Simon, M. Schmutz, P. J. Mesini, A. Banerjee, *Tetrahedron* **2008**, *64*, 175–185.
23. A. Carré, P. Le Grel, M. Baudy-Floc'h, *Tetrahedron Lett*. **2001**, *42*, 1887–1889.
24. S. H. Seo, J. Y. Chang, *Chem. Mater*. **2005**, *17*, 3249–3254.
25. A. R. Hirst, D. K. Smith, M. C. Feiters, P. M. Geurts, *Langmuir* **2004**, *20*, 7070–7077.
26. C. H. Tan, L. H. Su, R. Lu, P. C. Xue, C. Y. Bao, X. L. Liu, Y. Y. Zhao, *J. Mol. Liq*. **2006**, *124*, 32–36.
27. S. Kiyonaka, S. Shinkai, I. Hamachi, *Chem. Eur. J.* **2003**, *9*, 976–983.
28. A. D'Aléo, J.-L. Pozzo, F. Fages, M. Schmutz, G. Miedenbach-Gundert, F. Vögtle, V. Caplar, M. Zinić, C*hem. Commun.* **2004**, 190–191.
29. J. Makarević, M. Jokić, L. Frkanec, D. Katalenić, M. Zinić, *Chem. Commun*. **2002**, 2238–2239.
30. H. Ihara, T. Sakurai, T. Yamada, T. Hashimoto, M. Takafuji, T. Sagawa, H. Hachisako, *Langmuir* **2002**, *18*, 7120–7123.
31. S. Malik, S. K. Maji, A. Banerjee, A. K. Nandi, *J. Chem. Soc., Perkin Trans. 2* **2002**, *6*, 1177–1186.
32. S. Bhattacharya, Y. Krishnan-Ghosh, *Chem. Commun.* **2001**, 185–186.
33. A. Motulsky, M. Lafleur, A. C. Couffin-Hoarau, D. Hoarau, F. Boury, J. P. Benoit, J. C. Leroux, *Biomaterials* **2005**, *26*, 6242–6253.
34. D. J. Abdallah, R. G. Weiss, *Langmuir* **2000**, *16*, 7558–7561.
35. P. Terech, R. G. Weiss, *Chem. Rev*. **1997**, *97*, 3133–3160.
36. P. Terech, D. Pasquier, V. Bordas, C. Rossat, *Langmuir* **2000**, *16*, 4485–4494.
37. M. Suzuki, T. Sato, A. Kurose, H. Shirai, K. Hanabusa, *Tetrahedron Lett.* **2005**, *46*, 2741–2745.
38. W. D. Jang, D. L. Jiang, T. Aida, *J. Am. Chem. Soc*. **2000**, *122*, 3232–3233.
39. W. D. Jang, T. Aida, *Macromolecules* **2003**, *36*, 8461–8469.
40. C. Wang, D. Q. Zhang, D. B. Zhu, *J. Am. Chem. Soc*. **2005**, *127*, 16372–16373.

Povzetek

Zamislili smo si in pripravili nov organogelator, benzil (4-metil-1-okso-1-(2-heksadekanoilhidrazinil)pentan-2-il)karbamat (označen kot Cbz-Leu-HdHz). Ugotovili smo, da je ta spojina v mnogih organskih topilih zmožna samourejanja in termično reverzibilne tvorbe supramolekularnih organogelov. Temperaturo faznega prehoda gel-sol (T_{GS}) smo določili v odvisnosti od koncentracije gelatorja in iz tega določili ustrezne entalpije (ΔH_g). SEM, FT-IR in XRD analize smo uporabili za raziskavo morfologije in tvorbenih mehanizmov organogelov v prisotnosti Cbz-Leu-HdHz. Skladno z XRD podatki in molekularnim modeliranjem smo lahko predlagali načine pakiranje pri tvorbi agregatov organogelatorjev.